Oxidation of Porous Stainless Steel Supports for Metal-Supported Solid Oxide Electrolysis Cells

Fengyu Shen, Martha M. Welander, and Michael C. Tucker*

Energy Conversion Group, Lawrence Berkeley National Laboratory, Berkeley, CA 94720

Abstract

Oxidation behavior of porous P434L ferritic stainless steel, used for the fabrication of metal-supported solid oxide electrolysis cells (MS-SOEC), is studied under oxygen-side and steam-side conditions. The impact of oxygen content on the oxygen side and steam:hydrogen ratio on the steam side is determined at 700 °C for bare, as-sintered samples. For these conditions, oxidation is more aggressive in the steam-side atmosphere. Oxygen with 3% humidification and steam:hydrogen ratio of 90:10 are selected for further assessment with pre-oxidized, catalyst-coated, and $CuMn_{1.8}O_4$-coated samples. The rapid oxidation at 700 °C and breakaway oxidation at 600 °C observed for bare stainless steel in 90:10 steam:hydrogen is mitigated by pre-oxidizing the sample in air before exposure. In oxygen, addition of the catalyst or $CuMn_{1.8}O_4$ coatings moderately increases the oxidation rate, due to consumption of Cr via reaction between the coatings and Cr-oxide scale. The results for ex-situ controlled oxidation are similar to oxidation observed after 1000 h operation of a full MS-SOEC. In general, the oxidation behavior at 700°C is found to be acceptable.

Metal-supported; SOEC; electrolysis; oxidation; stainless steel

*mctucker@lbl.gov

Phone 1-510-486-5304

Fax 1-510-486-4260

LBNL; 1 Cyclotron Rd; MS 62-203; Berkeley CA 94720; USA

Introduction

Metal-supported solid oxide electrolysis cells (MS-SOECs) are being developed for steam electrolysis to produce green hydrogen. MS-SOECs are expected to be especially well suited for applications that require intermittent, dynamic, or aggressive operation, which are expected for utilization of variable renewable energy sources or waste heat [1-3]. The impact of these conditions on MS-SOEC durability have not yet been demonstrated, and the extent of oxidation of the metal supports in SOEC-relevant atmospheres is not well studied. The MS-SOEC concept and relevant atmospheres are depicted in Figure 1.

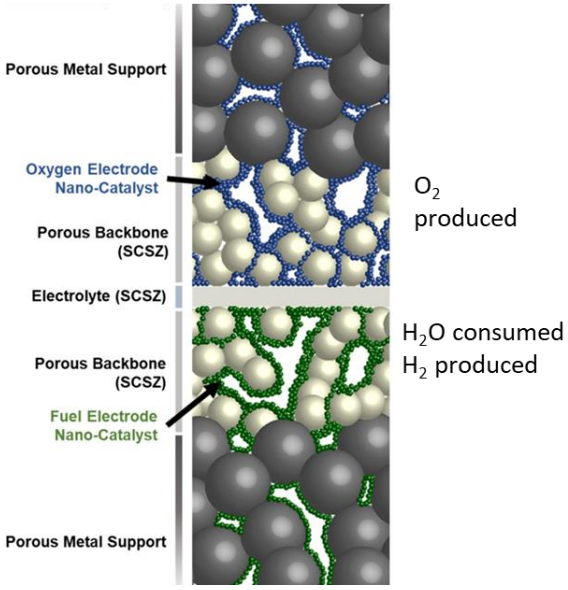

Figure 1. MS-SOEC design and SOEC-relevant atmospheres. Schematic of LBNL MS-SOEC design, adapted from Ref [9] with permission.

Oxidation of the metal supports is an inherent limitation of the MS-SOEC cell design, and selecting operating temperature and atmospheres, and coatings or treatments for the metal support that enable slow, protective growth of the Cr-oxide based scale is critical for long-term durability. A recent review of MS-SOECs pointed out that oxidation in high steam content is a concern, but most of the cell demonstrations to date have utilized a moderate steam:hydrogen ratio in the range 30:70 to 50:50, with only one report of 80:20 [4]. Steam content well above 80% is expected at the inlet of a SOEC stack, or during dynamic operation, however. Here, oxidation of porous metal supports in steam:hydrogen with a high steam content (75:25 and 90:10) is assessed. MS-SOECs produce pure oxygen on the oxygen evolution side, and oxidation in pure oxygen is known to be similar to that in air [5, 6]. In a real SOEC stack, however, some leaking between the oxygen and steam sides is expected to add humidity to the oxygen. Therefore, oxygen with 3% humidity is assessed here.

The Lawrence Berkeley National Laboratory (LBNL) MS-SOEC design utilizes P434L ferritic stainless steel on both sides [7-10]. The metal supports are pre-oxidized in air (850 °C, 10h) prior to catalyst infiltration to improve wetting of the aqueous solutions into the porous metal, and also to improve the oxidation resistance by forming a continuous protective Cr-based scale. The infiltrated catalysts are $La_{0.6}Sr_{0.4}Co_{0.2}Fe_{0.8}O_3$/$Ce_{0.8}Sm_{0.2}O_2$ (LSCF-SDC) for the oxygen evolution reaction and Ni/$Ce_{0.8}Sm_{0.2}O_2$ (SDCN, 60vol% SDC-40vol% Ni) for the steam reduction reaction. The impact of these treatments and catalyst coatings on oxidation of the porous supports has been studied in SOFC-relevant atmospheres, primarily ambient air and H_2O:H_2 with 55:45 ratio [11]. The oxidation rates and oxide scale composition were found to be acceptable for long-term durability in SOFC mode. More recently, addition of a $CuMn_{1.8}O_4$ coating on the oxygen side support was found to dramatically reduce transport of Cr from the metal support to the LSCF-SDC

[7], and this coating is now standard for our MS-SOECs. Here, oxidation of these metal supports in SOEC-relevant atmospheres is studied for the first time.

Experimental

Sample preparation

P434L porous stainless steel substrates were prepared by tape casting and sintering at 1350°C for 2 h in 2% H_2/98% Ar, to obtain samples with an approximate size of 1.5 cm x 1.5 cm x 0.35 mm and 40% porosity. The composition of the ferritic stainless steel alloy is listed in Table 1. "Bare" samples were used in the as-sintered state, without any further treatment. "Pre-oxidized" samples were exposed to ambient air at 850 °C for 10 h. "CMO coated" samples had a $CuMn_{1.8}O_4$ coating throughout the porous metal applied by electrophoretic deposition, as described in detail elsewhere [7]. Electrocatalysts were applied to some samples, using compositions and processes identical to those used for full MS-SOEC cells [7]. Pre-oxidized or CMO coated samples were additionally coated with 11 cycles of LSCF-SDC (6 LSCF and 5 SDC), and pre-oxidized samples were coated with 10 cycles of SDCN. The catalyst precursors were infiltrated with mild vacuum and converted to oxides in air for 30 min at 800 °C.

Fe	Cr	Mo	Si	Mn	P	C	S
Bal.	16.66	0.94	0.85	0.14	0.016	0.012	0.006

Table 1. Composition of P434L ferritic stainless steel (Ametek Specialty Metal Products).

Oxidation

Controlled oxidation was carried out in a tube furnace with alumina tube (Barnstead Thermolyne 21100). Samples were held vertically in an alumina sample holder in the hot zone of the furnace at 600, 700 or 800 °C. The ramping rate for heating and cooling was 7 °C/min. The tube furnace was calibrated prior to use and temperature deviated less than +/- 5 °C within the sample area. Metal flange caps (MTI) sealed the tube and had access ports for the inlet and outlet gas lines. The tube furnace exhaust was connected to a water bubbler to prevent backflow of air into the tube, and as a visual confirmation of chamber sealing. The flow rate of the dry gases was controlled with a mass flow controller (Alicat) to 100 sccm. The steam content was adjusted by bubbling the incoming gas (air, oxygen, or 2.8 % H_2 in Ar) through a distilled water bottle. These humidified atmospheres are referred to as "air", "oxygen", "75:25 H_2O:H_2", and "90:10 H_2O:H_2" throughout the text. For air and oxygen, the water bottle was exposed to ambient temperature, producing a steam content of approximately 3%. For 2.8 % H_2 in Ar, the water bottle was part of a humidification system (Fuel Cell Technologies), and the bottle temperature was controlled to 42.0 or 60.4 °C to produce either a 75:25 or 90:10 ratio of steam to hydrogen, respectively.

Weight gain is used here as an indicator of oxidation rate, as accurate calculation of oxidation rate kinetic constants for porous samples is notoriously difficult [11]. Weight gain is commonly used, and is useful for comparative purposes [12-20]. To measure the weight change, oxidation was interrupted after various time intervals by cooling the furnace to room temperature, weighing the samples, and re-heating to oxidation temperature. All samples were exposed to a total of 500 h at the oxidation temperature. To avoid condensation of water, samples were cooled with gas flowing from high temperature to 60°C (well above the dewpoint) and then quickly removed from the

furnace into open air. As a precautionary step, samples were further dried at 100 °C for 1 h before weight measurement to remove humidity from the porous surface. An analytical balance was used with a 0.01 mg accuracy (Ohaus Pioneer). The weight change is expressed as a weight increase per area, with the area being the superficial geometric area of the sample (~2.3 cm^2 and measured for each sample).

A full MS-SOEC cell was previously operated for 1000 h at 700 °C and 0.5 A cm^{-2} with ambient air and 50:50 H_2O:H_2, and details can be found elsewhere [7]. Oxidation of the supports after this operation was compared to the samples prepared here.

Characterization

After oxidation, surface morphologies and cross-sections of epoxy-mounted samples were observed by scanning electron microscopy (SEM) using a Zeiss Gemini Ultra-55 FESEM with an energy dispersive x-ray spectrometer (EDS).

Results and Discussion

The oxidation behavior of bare porous P434L at 700 °C was observed in humidified air, humidified oxygen, and steam/hydrogen mixtures with high steam content, in Section 1. The results guided selection of oxygen and 90:10 H_2O:H_2 atmospheres for more detailed study. Samples with various combinations of pre-oxidation treatment, CMO coating, and catalyst coatings were oxidized in these atmospheres and analyzed in Section 2. The impact of oxidation temperature in the range

600 to 800 °C was explored in Section 3. Breakaway oxidation was observed for 90:10 H_2O:H_2, and this was also explored in more detail in Section 3.

1. Oxidation of bare samples in various atmospheres

Bare P434L samples were oxidized at 700 °C in air, oxygen, 75:25 H_2O:H_2 and 90:10 H_2O:H_2, Figure 2. Weight gain is used as an indicator of oxide scale growth and relative oxidation rate, as the oxygen uptake in the oxidation processes dominates the evolution of the sample weight in these conditions. Specifically, at 700°C weight loss due to Cr evaporation is minimal compared to oxidation, and weight loss associated with oxide scale spallation is not expected to occur until the scale is several microns thick. In all atmospheres, a rapid initial oxidation in the first 90 h was followed by a slower weight gain, consistent with the linear-parabolic oxidation kinetics widely reported for porous ferritic stainless steels [13-15]. Air and oxygen produce similar oxidation behavior, as the growth rate of a continuous Cr_2O_3-based oxide scale is determined by the diffusion kinetics of Cr in the bulk alloy and oxygen in the scale, which are not affected by small variations in the oxygen partial pressure outside the scale [5]. Very large initial weight gain is observed for the H_2O:H_2 atmospheres, followed by long-term weight gain at a similar rate to air and oxygen. The initial weight gain is especially large for the higher steam content. This behavior is consistent with early breakaway oxidation, which shifts to protective oxidation once the surface is covered with oxide. The extent of oxidation observed here does not produce a measurable increase in sample volume. This is in contrast to full breakaway oxidation, which is discussed in more detail in Section 3.

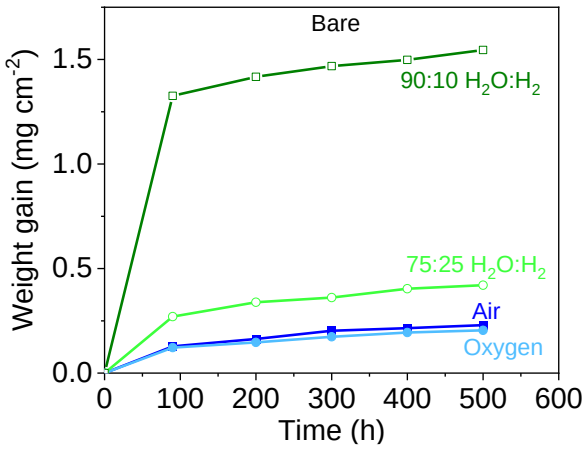

Figure 2. Oxidation in SOEC-relevant atmospheres. Oxidation of bare porous P434L supports at 700 °C. Weight gain during exposure to air (closed squares), oxygen (closed circles), 75:25 H_2O:H_2 (open circles), and 90:10 H_2O:H_2 (open squares).

The difference in oxidation behavior between the oxygen-side and steam-side atmospheres is elucidated by SEM observations, Figures 3 and S1-4. After 500 h oxidation in oxygen, the surface of the stainless steel is covered uniformly with a very thin Cr-oxide scale. Round Si-oxide particles with diameter of 1 to 2 μm are also scattered across the surface, and arise from the small amount of Si present in the P434L alloy, Table 1. A continuous layer of Si-oxide would impede electronic conduction between the stainless steel support and adjacent electrode and interconnect layers, but these small isolated particles are not expected to impact operation of the MS-SOEC. In a few locations, anomalous Ti-rich whiskers were observed. These are probably an artifact of using Ti powder as an oxygen getter in the sintering furnace, as some gas phase transport may occur. The oxide scale composition after 500 h oxidation in the 90:10 H_2O:H_2 atmosphere is quite different. The majority of the surface is coated with a Cr-oxide scale of variable thickness, which is generally

thicker than that observed in oxygen. Large regions are also covered with Fe-oxide crystals, consistent with breakaway oxidation. Large Si-rich patches up to about 20 μm wide are also observed, although these are discontinuous and therefore not expected to impede electronic conductivity. The oxide scale composition after 500 h oxidation in the 75:25 H_2O:H_2 atmosphere is more homogeneous than for the higher steam content. Fe-oxide crystals are not observed, and the Si-rich areas have less Si segregation and more uniform Si content. These observations are consistent with the lower oxidation rate observed for 75:25 H_2O:H_2 atmosphere.

Based on these initial results, oxygen and 90:10 H_2O:H_2 were selected for further studies. The high steam content was chosen because it was the most aggressive atmosphere. Oxygen was chosen because SOEC anodes are exposed to either pure oxygen or sweep air with elevated oxygen content, and oxidation of porous ferritic stainless steels in air is already well-studied.

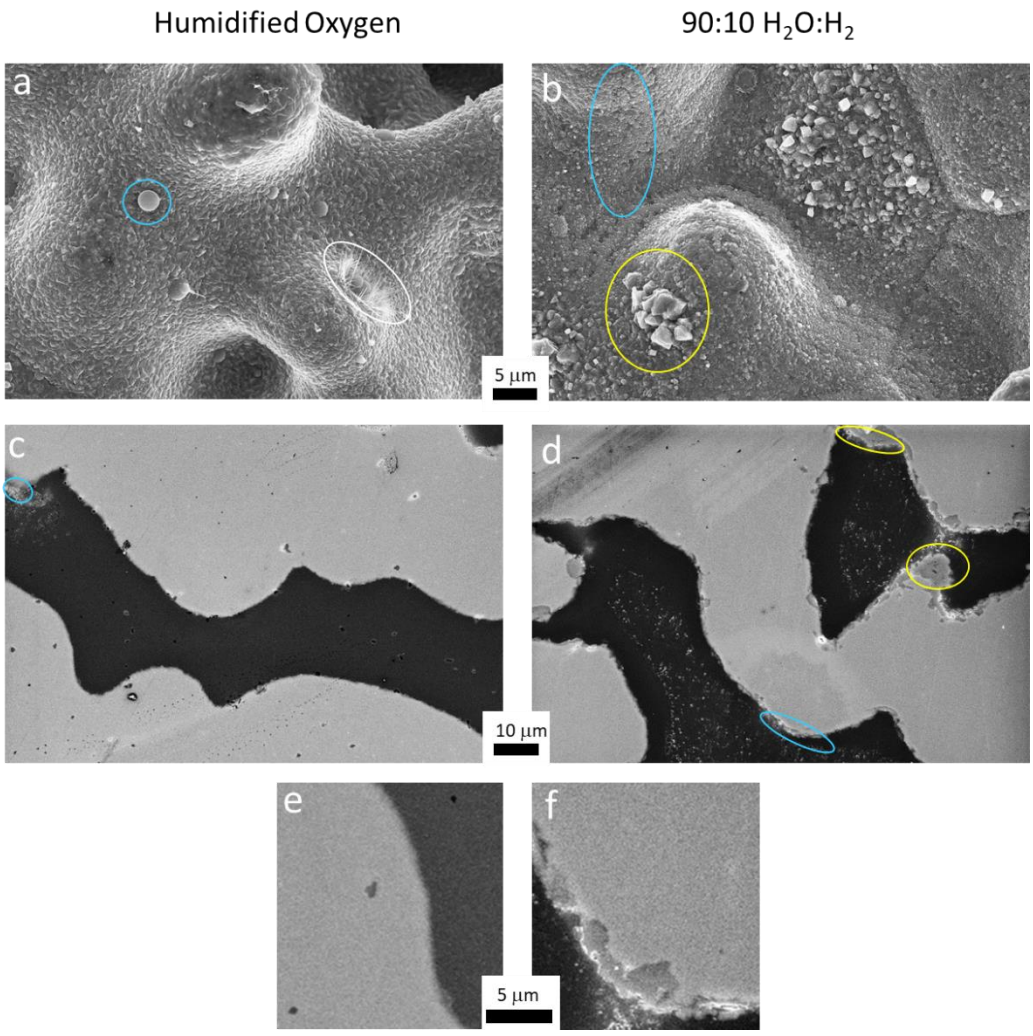

Figure 3. SEM analysis of bare samples after oxidation at 700 °C. (a,b) Surface images, (c,d) cross-section images, and (e,f) magnified cross-section images of bare samples after 500 h oxidation at 700 °C in (a,c,e) oxygen or (b,d,f) 90:10 H_2O:H_2. Si-rich (blue outline), Fe-rich (yellow outline), and Ti-rich (white outline) regions are highlighted. Cr-oxide scale is barely visible in (e) and appears as dark gray in (f).

2. Impact of pre-oxidation, coatings, and catalysts

Surface treatment of the bare stainless steel via pre-oxidation, CMO coating, and infiltration of LSCF-SDC or SDCN electrocatalysts significantly impacts oxidation behavior, Figure 4. Pre-oxidation of MS-SOC supports is a common method to prevent breakaway oxidation and lower the oxidation rate during operation [11, 16]. Generally, the as-sintered porous stainless steel is briefly oxidized in air or a mixture of steam and hydrogen at a temperature that is higher than the operating temperature. This treatment produces a thin conformal and stable protective oxide scale, typically predominantly Cr_2O_3, which prevents direct exposure of Fe and other elements in the bulk alloy to the operating atmosphere. Here, pre-oxidation occurs in air at 850 °C for 10 h. The pre-oxidation treatment dramatically reduces the oxidation rate for all atmospheres studied. This is a welcome result; although this effect is well-known, it has not been confirmed previously for porous supports at such high steam to hydrogen ratio, or in oxygen. Addition of SDCN to the pre-oxidized stainless steel further decreases the oxidation rate, consistent with previous results for 55:45 H_2O:H_2 [11]. In all cases, oxidation is faster in 90:10 H_2O:H_2 than in 75:25 H_2O:H_2, highlighting the concern for MS-SOECs operating with high inlet steam content (or MS-SOFCs with high fuel utilization). Oxidation in air and oxygen are similar, alleviating concern about the high oxygen content in MS-SOEC anodes.

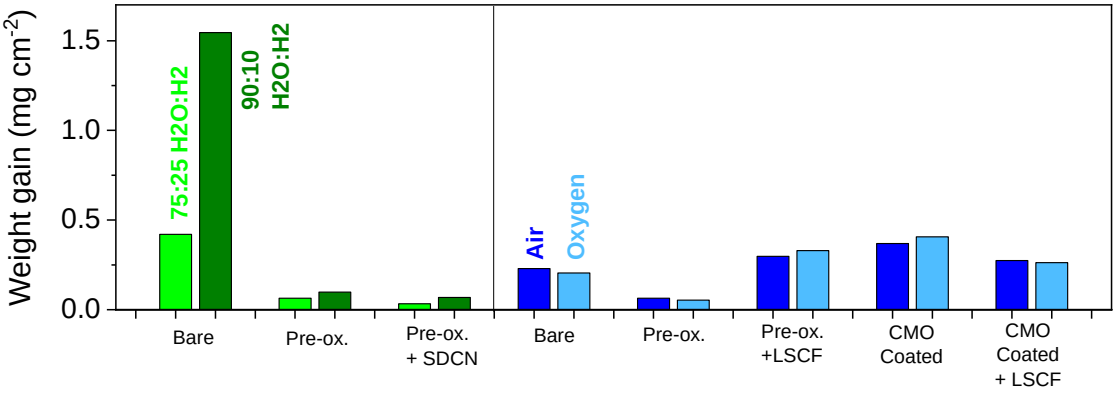

Figure 4. Oxidation of all samples at 700 °C. Weight gain after 500 h exposure at 700 °C in 75:25 H_2O:H_2 (light green), 90:10 H_2O:H_2 (dark green), air (dark blue), and oxygen (light blue). Samples were bare, pre-oxidized, pre-oxidized plus either LSCF (mixed with SDC) or SDCN, CMO coated, or CMO coated plus LSCF (mixed with SDC).

In contrast to the protection offered by SDCN, the addition of LSCF-SDC and CMO coatings increase the oxidation rate moderately. This is thought to arise from consumption of Cr from the oxide scale via reaction with LSCF and CMO, which reduces the scale's effectiveness in blocking oxygen diffusion to the bulk alloy. This is supported by post-oxidation SEM/EDS analysis, Figure 5. Cr is observed throughout the LSCF-SDC catalyst layer. Cr also clearly diffuses into the CMO coating (observed as a ~2 μm region of overlap of the Cu and Cr signals), consistent with a recent study of CMO on dense 430 stainless steel interconnects [21]. Furthermore, the CMO coated samples are not pre-oxidized before coating, and the post-coating treatment concludes with a 5 h annealing in air at 750 °C. Therefore, the initial protective scale is expected to be thinner and less effective than that produced by the pre-oxidation treatment (850 °C, 10 h). In contrast to the increased oxidation rate upon addition of LSCF-SDC to pre-oxidized stainless steel, when LSCF-SDC is added to a CMO-coated sample, the oxidation rate decreases. When LSCF is not in direct

contact with the Cr-oxide scale, it does not consume as much Cr, and the protective oxygen-blocking effect appears to outweigh the consumption of Cr. Indeed, the Cr/La ratio observed with the CMO coating (Fig 5b) is much less than that in the absence of the coating (Fig 5a).

Although the addition of CMO coating moderately increases the oxidation rate, it is very effective at blocking Cr migration from the stainless steel to LSCF-SDC, leading to dramatically improved performance and durability of MS-SOECs [7]. Nevertheless, it would be useful to identify coatings that suppress Cr migration without increasing the oxidation rate.

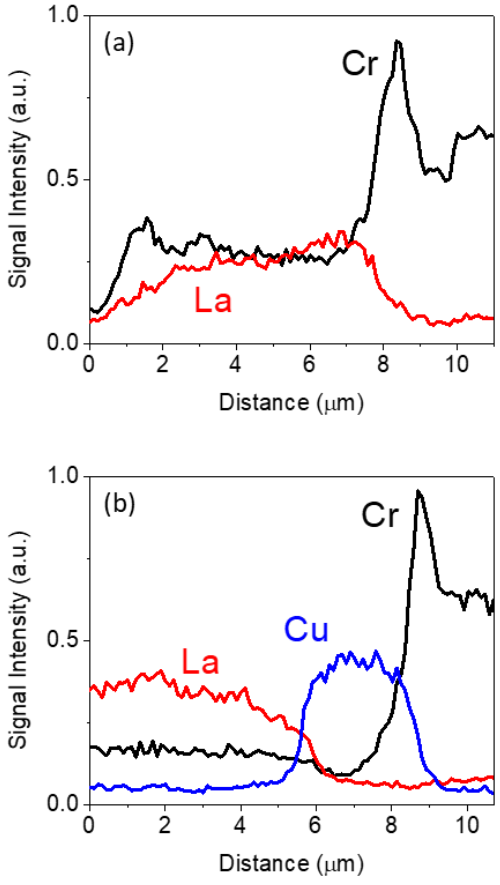

Figure 5. Cr accumulation in LSCF after 500 h oxidation at 700 °C in oxygen. SEM/EDS line scans from the pore space (filled with LSCF-SDC) into the bulk alloy. (a) Pre-oxidized plus LSCF-SDC and (b) CMO coating plus LSCF-SDC.

As a comparison to the free-standing metal supports studied here, the oxidation of metal supports harvested from a full cell MS-SOEC after 1000 h operation was observed, Figure 6. The operating atmospheres (ambient air and 50:50 H_2O:H_2) were different than the more aggressive atmospheres studied here, and the timescale differed, but the general observations are consistent. Based on the Cr-scale thickness, the oxidation rate is higher on the oxygen side than on the steam side. Cr migration into the CMO coating is observed. A thin Si-oxide sub-scale is formed, but it is not continuous, so electronic conduction is maintained (see Figure S5). These observations increase our confidence that the ex-situ oxidation studies are relevant to the oxidation actually occurring in an operating MS-SOEC.

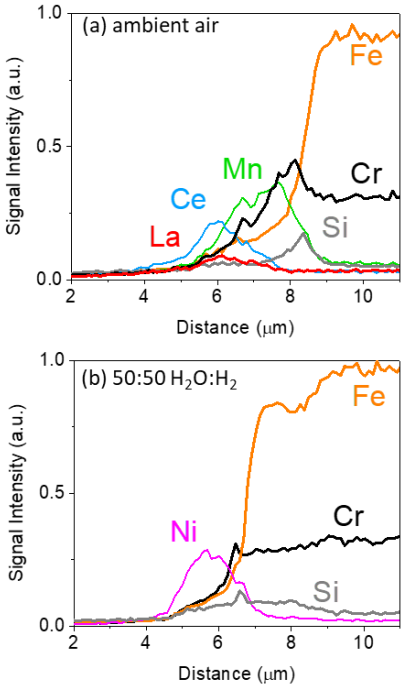

Figure 6. Elemental analysis of porous metal supports after operating in a full cell for 1000 h at 700 °C and 0.5 A cm^{-2} with ambient air and 50:50 H_2O:H_2. EDS line scans from the pore space (containing LSCF-SDC or SDCN electrocatalysts) into the bulk alloy. (a) Oxygen-side support with CMO coating and LSCF-SDC and (b) steam-side support with SDCN. EDS maps are shown in Figure S5.

3. Impact of oxidation temperature

The anticipated operation temperature for MS-SOECs is around 700 °C, however thermal excursions may cause higher temperature, and if the performance is significantly improved then a lower operating temperature would be desirable. Therefore, oxidation at 600 and 800 °C was also assessed, Figure 7. Oxidation is moderately slower at 600 °C and significantly faster at 800 °C than at 700 °C, consistent with the Arrhenius kinetics of stainless steel oxidation [22]. For oxygen, pre-oxidation reduces the oxidation rate at all temperatures, Figure 7a. At 600 °C, the weight gain was actually negative due to weight loss via Cr evaporation being faster than weight gain via oxygen uptake at this low temperature. This phenomenon has been observed in the temperature range 550 to 650 °C [11, 23]. The trend of increased oxidation with CMO coating and LSCF-SDC catalysts discussed for 700 °C (Section 2) is exacerbated here at 800 °C, presumably due to increased migration and reaction of Cr with those coatings. For 90:10 H_2O:H_2 at all temperatures, pre-oxidation significantly reduces the oxidation rate and addition of SDCN moderately reduces it further, Figure 7b. These features are similar to the results reported previously for bare and coated porous P434L samples in SOFC conditions [11].

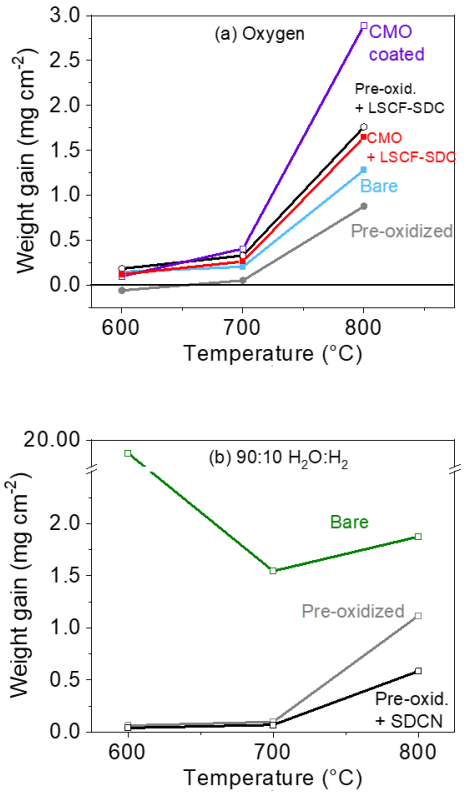

Figure 7. Impact of oxidation temperature. Weight gain after 500 h oxidation in (a) oxygen or (b) 90:10 H_2O:H_2 for various samples.

Severe breakaway oxidation is observed for bare stainless steel at 600 °C in 90:10 H_2O:H_2. This oxidation mode occurs when Cr consumption via oxidation is faster than Cr diffusion from the bulk to the surface, resulting in rapid formation of Fe-oxides and (Fe,Cr)-oxides [24, 25]. A protective Cr-rich scale is not formed, and the results are catastrophic: the pores of the metal support become filled with oxides, Figures 8a and S6, and expansion of the metal support can lead to cracking of the electrolyte and cell failure [26]. Breakaway oxidation is especially problematic around 600 °C. At 700 °C, only localized formation of Fe-oxides is observed, Figure 3d, and at 800 °C no Fe-oxide is observed, Figures 8b and S6. Pre-oxidation (with or without SDCN addition)

completely prevents breakaway oxidation, even in the aggressive 90:10 H_2O:H_2 atmosphere, as a continuous protective Cr-oxide scale is formed before exposure, Figures 7b and S6. Breakaway oxidation was not observed in oxygen for any sample or temperature. This is consistent with previous results for air with low humidity, but breakaway oxidation is expected for bare metal if the humidity level is significantly higher (10% or more) for example due to a leak [11].

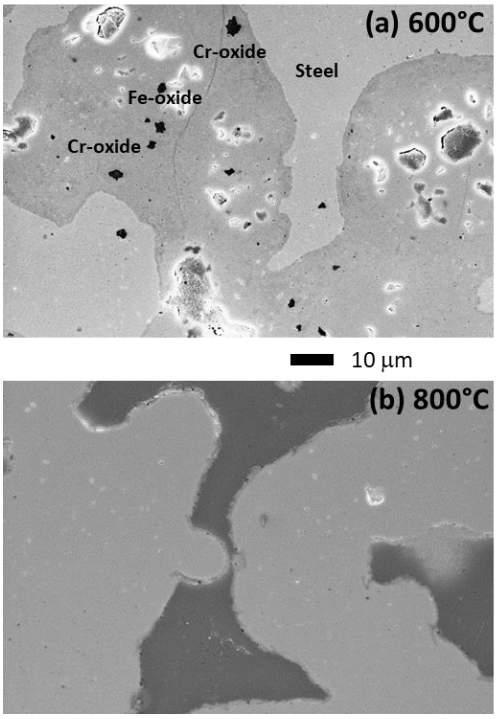

Figure 8. Breakaway oxidation. SEM cross-section images of bare samples oxidized for 500 h in 90:10 H_2O:H_2 at (a) 600 °C and (b) 800 °C. For (a), the light gray area is bulk alloy, and the darker gray porous area is a mixture of Fe-oxides and (Cr,Fe)-oxides. Fig 3d is a comparable image for 700 °C. Corresponding EDS maps are shown in Fig S6.

Conclusions

Oxidation behavior in atmospheres relevant to SOEC operation was assessed for porous ferritic stainless steel P434L. For bare and pre-oxidized stainless steel, 90:10 H_2O:H_2 is more aggressive than oxygen. Breakaway oxidation was exacerbated by the high steam content in 90:10 H_2O:H_2 atmosphere, and was mild at 700 °C but catastrophic at 600 °C. Pre-oxidation in air before exposure to the aggressive steam/hydrogen atmosphere was effective at preventing breakaway oxidation. Adding Cr-blocking and electrocatalyst coatings that consume Cr from the oxide scale moderately increases the oxidation rate in oxygen. Results for the ex-situ samples studied here are consistent with oxidation observed in an MS-SOEC operated for 1000 h. It is recommended that the maximum long-term operating temperature for MS-SOECs be limited to approximately 700 °C. The results for SOEC-relevant atmospheres shown here are broadly similar to those observed previously for SOFC-relevant atmospheres. This work further increases confidence that porous ferritic stainless steel supports with appropriate treatments or coatings are suitable for MS-SOECs, by demonstrating acceptable oxidation behavior with coatings and atmospheres that are specific to MS-SOEC operation.

Acknowledgements

The authors gratefully acknowledge research support from the HydroGEN Advanced Water Splitting Materials Consortium, established as part of the Energy Materials Network under the U.S. Department of Energy, Office of Energy Efficiency and Renewable Energy, Fuel Cell Technologies Office, under Contract Number DE-AC02-05CH11231. The use of Zeiss Gemini Ultra-55 FESEM in the Molecular Foundry of Lawrence Berkeley National Laboratory was supported by the Office of Science, Office of Basic Energy Sciences, of the U.S. Department of

Energy under Contract No. DE-AC02-05CH11231. This work was funded in part by the U.S. Department of Energy under contract no. DE-AC02-05CH11231. The views and opinions of the authors expressed herein do not necessarily state or reflect those of the United States Government or any agency thereof. Neither the United States Government nor any agency thereof, nor any of their employees, makes any warranty, expressed or implied, or assumes any legal liability or responsibility for the accuracy, completeness, or usefulness of any information, apparatus, product, or process disclosed, or represents that its use would not infringe privately owned rights.

References

[1] Krishnan VV. Recent developments in metal-supported solid oxide fuel cells. Wiley Interdisciplinary Reviews: Energy and Environment. 2017;6:e246.
[2] Larring Y, Fontaine M-L. Critical Issues of Metal-Supported Fuel Cell. 2013:71-93.
[3] Tucker MC. Progress in metal-supported solid oxide fuel cells: A review. Journal of Power Sources. 2010;195:4570-82.
[4] Tucker MC. Progress in metal-supported solid oxide electrolysis cells: A review. International Journal of Hydrogen Energy. 2020;45:24203-18.
[5] Alnegren P, Sattari M, Froitzheim J, Svensson JE. Degradation of ferritic stainless steels under conditions used for solid oxide fuel cells and electrolyzers at varying oxygen pressures. Corrosion Science. 2016;110:200-12.
[6] Palcut M, Mikkelsen L, Neufeld K, Chen M, Knibbe R, Hendriksen PV. Corrosion stability of ferritic stainless steels for solid oxide electrolyser cell interconnects. Corrosion Science. 2010;52:3309-20.
[7] Shen F, Reisert M, Wang R, Singh P, Tucker MC. Assessment of Protective Coatings for Metal-Supported Solid Oxide Electrolysis Cells. ACS Applied Energy Materials. 2022;5:9383-91.
[8] Shen F, Wang R, Tucker MC. Long term durability test and post mortem for metal-supported solid oxide electrolysis cells. Journal of Power Sources. 2020;474:228618.
[9] Wang R, Dogdibegovic E, Lau GY, Tucker MC. Metal-Supported Solid Oxide Electrolysis Cell with Significantly Enhanced Catalysis. Energy Technology. 2019;7:1801154.
[10] Wang R, Lau GY, Ding D, Zhu T, Tucker MC. Approaches for co-sintering metal-supported proton-conducting solid oxide cells with Ba(Zr,Ce,Y,Yb)O3-δ electrolyte. International Journal of Hydrogen Energy. 2019;44:13768-76.
[11] Reisert M, Berova V, Aphale A, Singh P, Tucker MC. Oxidation of Porous Stainless Steel Supports for Metal-Supported Solid Oxide Fuel Cells. International Journal of Hydrogen Energy. 2020;Submitted.
[12] Jeong H, Roehrens D, Bram M. Facile route for reactive coating of LaCrO3 on high-chromium steels as protective layer for solid oxide fuel cell applications. Materials Letters. 2020;258:126794.
[13] Molin S, Gazda M, Jasinski P. High temperature oxidation of porous alloys for solid oxide fuel cell applications. Solid State Ionics. 2010;181:1214-20.
[14] Molin S, Gazda M, Jasinski P. Coatings for improvement of high temperature corrosion resistance of porous alloys. Journal of the European Ceramic Society. 2011;31:2707-10.

[15] Reiss G, Frandsen HL, Persson ÅH, Weiß C, Brandstätter W. Numerical evaluation of oxide growth in metallic support microstructures of Solid Oxide Fuel Cells and its influence on mass transport. Journal of Power Sources. 2015;297:388-99.
[16] Stange M, Denonville C, Larring Y, Brevet A, Montani A, Sicardy O, et al. Improvement of corrosion properties of porous alloy supports for solid oxide fuel cells. International Journal of Hydrogen Energy. 2017;42:12485-95.
[17] Stange M, Stefan E, Denonville C, Larring Y, Rørvik PM, Haugsrud R. Development of novel metal-supported proton ceramic electrolyser cell with thin film BZY15–Ni electrode and BZY15 electrolyte. International Journal of Hydrogen Energy. 2017;42:13454-62.
[18] Stefan E, Denonville C, Larring Y, Stange M, Haugsrud R. Oxidation study of porous metal substrates for metal supported proton ceramic electrolyzer cells. Corrosion Science. 2020;164:108335.
[19] Yan Y, Bateni R, Harris J, Kesler O. Fabrication of reactive element oxide coatings on porous ferritic stainless steel for use in metal-supported solid oxide fuel cells. Surface and Coatings Technology. 2015;272:415-27.
[20] Sarasketa-Zabala E, Otaegi L, Rodriguez-Martinez LM, Alvarez MA, Burgos N, Castro F, et al. High temperature stability of porous metal substrates under highly humidified hydrogen conditions for metal supported Solid Oxide Fuel Cells. Solid State Ionics. 2012;222-223:16-22.
[21] Zhu Z, Darl-Uzu C, Pal U, Gopalan S, Hussain AM, Dale N, et al. Comparison of Cu–Mn and Mn–Co spinel coatings for solid oxide fuel cell interconnects. International Journal of Hydrogen Energy. 2022.
[22] Karczewski J, Brylewski T, Miruszewski T, Andersen KB, Jasinski PZ, Molin S. High-temperature kinetics study of 430L steel powder oxidized in air at 600–850 °C. Corrosion Science. 2019;149:100-7.
[23] Falk-Windisch H, Svensson JE, Froitzheim J. The effect of temperature on chromium vaporization and oxide scale growth on interconnect steels for Solid Oxide Fuel Cells. Journal of Power Sources. 2015;287:25-35.
[24] Young DJ, Zurek J, Singheiser L, Quadakkers WJ. Temperature dependence of oxide scale formation on high-Cr ferritic steels in Ar–H2–H2O. Corrosion Science. 2011;53:2131-41.
[25] Żurek J, Wessel E, Niewolak L, Schmitz F, Kern TU, Singheiser L, et al. Anomalous temperature dependence of oxidation kinetics during steam oxidation of ferritic steels in the temperature range 550–650 °C. Corrosion Science. 2004;46:2301-17.
[26] Dogdibegovic E, Wang R, Lau GY, Karimaghaloo A, Lee MH, Tucker MC. Progress in durability of metal-supported solid oxide fuel cells with infiltrated electrodes. Journal of Power Sources. 2019;437:226935.